Development of a Forceps Force Limiter Using Leaf Spring Buckling

Satsuya Noda (snoda@fukushima-nct.ac.jp)

Department of Mechanical System Engineering, National Institute of Technology, Fukushima College, 30 Tairakamiarakawa-aza-Nagao, Iwaki, 970-8034 Fukushima, Japan

Research Article

Keywords: Buckling, Forceps, Force limiter

Posted Date: February 4th, 2020

DOI: https://doi.org/10.21203/rs.2.22608/v1

RESEARCH

Development of a Forceps Force Limiter Using Leaf Spring Buckling

Satsuya Noda*

Abstract

To prevent accidents in minimally invasive surgeries, force limiters have been developed for forceps grippers. When a force limiter is in use, if the absolute value of its spring constant is reduced, the risk of damage to the organs decreases. This paper proposes the use of a leaf spring buckling mechanism as a force limiter for forceps. The results obtained indicate that the spring constant of a buckled leaf spring is lower than that of a normal coil spring. Furthermore, the use of a leaf spring allows the independent adjustment of its thickness and width, based on the stress and force values. This enables an easy calibration of the threshold value. In the experiments, the spring constant of the buckled leaf spring was 1.5×10^{-1} N/mm, which is half of that of a normal coil spring. After calibrating the gripping force, it was confirmed that the force limiter reduced the extent of damage to the dummy organs in the ex vivo experiments.

Keywords: Buckling; Forceps; Force limiter

Introduction

An advantage of minimally invasive surgery (MIS) is the reduction of damage to the patient after the surgery; however, this type of surgery requires difficult techniques by surgeons as compared to conventional surgery. The degree of freedom in general surgical instruments decreases from six to four because these instruments are inserted into trocars. Hence, surgical robots [1] or manipulators [2] have been developed.

One problem with these surgical instruments is the transmission of force information. Some surgical robots [1] lose the force information to the surgeons. Even though surgical manipulators with force feedback are used, surgeons with little experience in MIS have difficulty controlling the force acting on the instruments. Applying excess force in gripping or exclusion might cause serious damage to the organs. To prevent such accidents, it is generally effective to measure the force acting on the forceps; thus, many force sensors have been developed for forceps [3, 4, 5]. However, equipping forceps only with force sensors does not eliminate accidents owing to the use of excess force.

To prevent such accidents, force limiters for forceps [6, 7, 8] have been developed. If the gripping force exceeds the threshold value, the coil spring begins to deform, as shown in Fig. 1. Because a normal force limiter employs a linear coil spring, the gripping force increases proportionally to the handle displacement, which might cause damage to the gripped organ. On the other hand, if the spring force decreases with the displacement, the gripping force decreases, which might cause the organ to slip from the gripper. Therefore, to decrease the change in force with respect to the displacement, the absolute value of the spring constant of a force limiter should be low.

To reduce the spring constant without changing the threshold value of the force limiter, the number of windings of a coil spring should be increased. However, such springs will require more length and installing them for the gripper will become difficult. Although a constant load spring or a coil spring with a noncircular pulley [9] can be employed to reduce the spring constant, the size of this spring will pose difficulties in attaching it to the gripper.

This paper proposes the use of a leaf spring buckling mechanism as a force limiter for forceps. The spring constant of the buckled leaf spring is lower than that of a normal coil spring. Previous studies have examined mechanisms that use buckling; for example, some personal computer keyboards employ buckled coil springs [10], leaf springs are used in constant load springs [11], and a force limiter for a toothbrush employs a leaf spring [12]. Compared to previous studies, the advantage of this study is the ease of adjusting the design parameters. The use of a leaf spring allows

Correspondence: snoda@fukushima-nct.ac.jp
Department of Mechanical System Engineering, National Institute of Technology, Fukushima College, 30 Tairakamiarakawa-aza-Nagao, Iwaki, 970-8034 Fukushima, Japan
Full list of author information is available at the end of the article
*Equal contributor

the independent adjustment of its thickness and width, based on the stress and force values.

Force limiter mechanism

Figure 2 shows the mechanism of the proposed force limiter. The handle of the force limiter consists of base and movable handles. Generally, the movable handle is used for gripping, whereas the base handle does not move. If the gripper of the distal side grasps an organ and the movable handle rotates in the gripping direction, the gripping force increases. Hence, the gripping force will not increase if the gripper of the distal side does not rotate. In the prototype model of the force limiter, the ease of a leaf spring attachment is significant. Thus, this study proposes the base handle mechanism that moves only when the gripping force exceeds the threshold value. If the base handle can be driven by a constant force, the gripping force will not increase (see Fig. 2 (b)). The use of the leaf spring buckling enables to prevent the gripping force increase. Furthermore, the linkage mechanism of the base handle also assists in preventing the gripping force increase.

Leaf spring buckling

Figure 3 shows the coordinate system of the leaf spring. The bending formula is given by the following expression:

$$\kappa(s) = \theta'(s) = -\frac{M(s)}{EI}, \tag{1}$$

where s is the arc length from the edge, $x(s)$ and $y(s)$ indicate the position of the leaf spring at s, $\theta(s)$ is the angle of the tangential line from the x-axis at s, $'$ denotes the derivative with respect to s, $\kappa(s)$ is the curvature at s, $M(s)$ is the bending moment at s, E is the Young's modulus of the leaf spring, and I is the moment of inertia of the cross-sectional area of the leaf spring.

Because the cross section of the leaf spring is a rectangle, I is given by

$$I = \frac{bt^3}{12}, \tag{2}$$

where b and t denote the width and thickness of the leaf spring, respectively.

$M'(s)$ denotes the shearing force at s. By differentiating (1), the following equation is obtained:

$$\frac{d^2\theta(s)}{ds^2} = -A\sin\theta \tag{3}$$

$$A = \frac{F_b}{EI}, \tag{4}$$

where F_b denotes the buckling load.

Equation (3) is analogous to the equation of motion of a nonlinear pendulum, whereby the buckling load corresponds to the period of the pendulum. Let $\theta_{\max}$ be $\mathrm{Max}|\theta(s)|$. It is known that the period of a nonlinear pendulum is given by the complete elliptic integral of the first kind and depends on $\theta_{\max}$ [13]. This study assumes $\theta_{\max} \leq 45$ °, as described in the Simulation section. In this range, the period error of a nonlinear pendulum is less than 5 % of that of a linear pendulum. Similarly, the buckling load error of a nonlinear deformation is less than 10 % of that of a linear deformation.

The buckling load of a linear deformation is given by the following equation:

$$F_b = c\pi^2\frac{EI}{l^2}, \tag{5}$$

where l denotes the length of the leaf spring and c denotes the coefficient of fixity. From (2) and (5), it is obvious that b can be used to adjust F_b because $F_b \propto I \propto b$.

The coefficient c is determined as follows:
(a) $c = 1$, if both edges cannot support momentum loads (see Fig. 4 (A)).
(b) $c = 4$, if both edges can support momentum loads (see Fig. 4 (B)).
Because the proposed force limiter can support the moment of the buckling direction, as shown in Fig. 2, the procedure for this study sets $c = 4$.

Design procedure for the force limiter mechanism

Because the spring constant of the buckled leaf spring is lower than that of a normal coil spring, it is difficult to analyze the stress produced by the load. The analysis of this stress requires the calculation of the leaf spring deformation. Therefore, the parameters are determined in the order of l, t, and b. Considering the handle size, the parameters were set so as to minimize l. A detailed description of each step in the design of the leaf spring is given below:

Step 1: Determine the range of L_3 and L_4.

Let F_{in} be the input force to the linkage and Δx_{in} be the base handle displacement in the x direction. This step provides F_{in} and Δx_{in}. The designed buckling load F_i and displacement of the leaf spring Δx_i are calculated using

$$F_i = \frac{L_{3i}}{L_{4i}}F_{\mathrm{in}} \tag{6}$$

$$\Delta x_i = \frac{L_{4i}}{L_{3i}}\Delta x_{\mathrm{in}}. \tag{7}$$

L_{3i} and L_{4i} are determined using

$$L_{3i} = L_{3\min} + \frac{L_{3\max} - L_{3\min}}{m_1} i \quad (8)$$

$$L_{4i} = L_2 - L_{3i}, \quad (9)$$

where $i = 0,\ 1 \ldots m_1$. In this range, the value of L_3 that minimized l is determined.

Step 2: Determine the range of l.

Let l_i be the value of l that corresponds to L_{3i} and L_{4i}. From the leaf spring length limitation, l_i must satisfy $l_i > \Delta x_i$. $l_{\max}$ denotes the maximum length, which is limited by the handle size. Thus, $l_i \leq l_{\max}$. Hence, l must be sampled in the range $\Delta x_i < l \leq l_{\max}$. Let l_{ij} be the jth sample of l_i. Then, $l_{ij} = \Delta x_i + \frac{l_{\max} - \Delta x_i}{m_2} j$, where $j = 0, 1 \ldots m_2$. In Step 2, $j = 0$.

Step 3: Simulate the deformed shape.

The linear constitutive relationship is given by

$$\begin{bmatrix} x'(s) \\ y'(s) \end{bmatrix} = \begin{bmatrix} \cos\theta(s) \\ \sin\theta(s) \end{bmatrix}, \quad (10)$$

where the initial conditions are as follows:

$$(x(0),\ y(0)) = (0,\ 0) \quad (11)$$

$$\theta(0) = \mathrm{atan2}(y'(0), x'(0)) \quad (12)$$

$$(x'(0),\ y'(0)) = (1,\ 0). \quad (13)$$

The boundary conditions are as follows:

$$(x(l_{ij}),\ y(l_{ij})) = (l_{ij} - \Delta x_i,\ 0) \quad (14)$$

Equations (3) and (10) are solved by a numerical method, such as the Runge–Kutta method. Let A_{ij} be A with respect to l_{ij}. To satisfy the boundary conditions, these calculations are nested within the adjustment procedure loop of A_{ij} and $\kappa(0)$. To increase the convergence precision, the adjustment procedure is described as follows:

Loop 1: Let ε be the allowable error of the edge position. The procedure adjusts A_{ij}, which satisfies $|y(l_{ij})| < \varepsilon$. An optimization process is used to determine A_{ij}.

Loop 2: The procedure adjusts $\kappa(0)$, which satisfies $|x(l_{ij}) - (l_{ij} - \Delta x_i)| < \varepsilon$. If $\kappa(0)$ is updated, then Loop 1 is performed.

Step 4: Determine the range of t at l_{ij}.

The constraints on t are described as follows:

(a) The lower limit of t

Let $t_{\min}$ be the lower limit of t and $t \geq t_{\min}$.

(b) The maximum stress

Let $\sigma(s)$ be the maximum stress at s, then $|\sigma(s)|$ is given by

$$|\sigma(s)| = \frac{|M(s)|}{Z}, \quad (15)$$

where Z denotes the modulus of the section, which is given by

$$Z = \frac{bt^2}{6}. \quad (16)$$

From (1), (2), (15), and (16), $\sigma(s)$ is calculated by the following equation that does not include $M(s)$:

$$|\sigma(s)| = \frac{|\kappa(s)|Et}{2}. \quad (17)$$

According to (17), $\sigma(s)$ does not depend on b but depends on $\kappa(s)$, E, and t. Let $\sigma_{\lim}$ be the proof stress. Because $|\sigma(s)| \leq \sigma_{\lim}$, t must satisfy

$$t \leq \frac{2\sigma_{\lim}}{E\kappa_{\max}}, \quad (18)$$

where

$$\kappa_{\max} = \mathrm{Max}|\kappa(s)|. \quad (19)$$

(c) The limitation of b

From (2) and (5), if t is determined, then b can be calculated by

$$b = \frac{12 l_{ij}^2 F_i}{c\pi^2 E t^3}. \quad (20)$$

Let $b_{\max}$ be the maximum b, which is determined by the gripper size. Then b must satisfy $b \leq b_{\max}$, thus

$$t \geq \sqrt[3]{\frac{12 l_{ij}^2 F_i}{c\pi^2 b_{\max} E}}. \quad (21)$$

If $t > b$, then (20) cannot be used to determine b because the buckling direction in this case is orthogonal to the direction shown in Fig. 2. Hence, to satisfy $t \leq b$, t must satisfy

$$t \leq \sqrt[4]{\frac{12 l_{ij}^2 F_i}{c\pi^2 E}}. \quad (22)$$

Let t_{ijk} be t with respect to l_{ij}. Hence, t_{ijk} must satisfy

$$t_{ij\alpha} \leq t_{ijk} \leq t_{ij\beta}, \quad (23)$$

where $k = 0, 1 \ldots n_{ij}$ $(n_{ij} < (t_{ij\beta} - t_{ij\alpha})/\Delta t)$,

$$t_{ijk} = t_{ij\beta} - k\Delta t \quad (24)$$

$$t_{ij\alpha} = \max\left(t_{\min}, \sqrt[3]{\frac{12 l_{ij}^2 F_i}{c\pi^2 b_{\max} E}}\right) \quad (25)$$

$$t_{ij\beta} = \min\left(\frac{2\sigma_{\lim}}{E\kappa_{\max}}, \sqrt[4]{\frac{12 l_{ij}^2 F_i}{c\pi^2 E}}\right). \quad (26)$$

The procedure sets $\Delta t = 0.1$ mm, which is the thickness of a commonly available plate. In Step 3, $k = 0$. If $t_{ij\alpha} > t_{ij\beta}$, then the procedure is described as follows:
(a) If $j < m_2$, the procedure increases j by one and returns to Step 3.
(b) If $j = m_2$, the procedure excludes ith candidate.

Step 5: Determine b_{ijk}.

Let b_{ijk} be b at t_{ijk}, then b_{ijk} is calculated from (20).

Step 6: Final stress confirmation.

The maximum $|\sigma(s)|$ obtained by (17) is a little less than that obtained by the finite element method (FEM). Therefore, the final stress confirmation is conducted by the FEM. Let $\sigma_{\max}$ be the maximum stress obtained by the FEM. Because the leaf spring buckles symmetrically, the half-size analysis can decrease the calculation time. If $\sigma_{\max} \leq \sigma_{\lim}$, then the leaf spring design is completed. If $\sigma_{\max} > \sigma_{\lim}$, then the procedure is described as follows:
(a) If $k < n_{ij}$, the procedure increases k by one and returns to Step 5.
(b) If $k = n_{ij}$ and $j < m_2$, the procedure sets $k = 0$, which increases j by one and returns to Step 3.
(c) If $k = n_{ij}$ and $j = m_2$, the procedure excludes ith candidate.

Step 7: Candidate selection.

In this step, the minimum value of l_{ij} is selected. If there are no candidates of l_{ij} remaining, then the procedure returns to Step 1 and the values of F_{in} and Δx_{in} are modified.

Simulations and experiments

Spring constant of the buckled leaf spring

The spring constant of the buckled leaf spring was confirmed through simulations and experiments. Strong surgical stainless steel (SUS631, with Young's modulus of 200 GPa, Poisson's ratio of 0.28 and $\sigma_{\lim} = 1030$ MPa (proof stress)) was selected as the material for the leaf spring. In this study, it was assumed that the gripping force of the distal side is equal to that of the proximal side. Referring to the maximum range of the force sensor [14], the gripping force of the force sensor was set as $F_{\text{in}} = 6$ N. The linkage parameters were set as $(L_1, L_2) = (2, 60)$ mm. The minimum thickness of the commonly available plate was set as $t_{\min} = 0.1$ mm. The values of $l_{\max}$ and $b_{\max}$ were set as 180 mm and 30 mm, respectively; these values were determined with reference to the length of the middle finger and half the length of the thumb, according to the database of Japanese hand sizes [14]. The range of L_3 was set as $(L_{3\min}, L_{3\max}) = (24, 36)$ mm. These values were determined based on the length of L_2. Δx_{in} is set as 8.0 mm. SolidWorks 2016 was used to implement the FEM for the stress analysis.

Table 1 shows the candidates of L_3 and L_4. The value of l was the smallest for the 4th candidate, i.e., 50 mm. The linkage parameters were set as $(L_3, L_4) = (33, 27)$ mm. Table 2 shows the specifications of the leaf spring. Figure 5 and Table 3 show the deformed shape of the leaf spring with $\Delta x_i = 6.5$ mm; this simulation converged to $(x(l), y(l)) = (43.5, 0)$ mm and $(x'(l), y'(l)) = (1, 0)$. Using the FEM, $\sigma_{\max} = 997$ MPa, which is lower than $\sigma_{\lim}$ (see Fig. 6) . From Fig. 6, little difference of the stress was observed in the width direction.
Note: This procedure adjusted the value of L_1 to minimize the absolute value of the spring constant of the leaf spring.

Furthermore, the spring constant of the leaf spring was confirmed by experiments. Figure 7 shows the experimental setup for the force measurement. A force gauge (AIKOH model RZ-20) was attached on a linear stage, which deformed the leaf spring. To separate the force gauge from the momentum load, the leaf spring was fixed to the arm device as shown in Fig. 7.
Note: In the experiments, a stage of a milling machine (TOYO ASSOCIATES: Little Milling 9) was used instead of a linear stage.

Figure 8 shows the result of the leaf spring buckling experiment. From the simulation results, the spring constant of the leaf spring was estimated to be 7.9×10^{-2} N/mm, which is about two-sevenths of that of a weak coil spring (2.8×10^{-1} N/mm for the MISUMI AWA 8-30 spring of outer diameter 8 mm, length 50 mm at 6.7 N, and maximum load of 8.53 N). From the experimental results, the spring constant was estimated as 1.5×10^{-1} N/mm in the range $0.5 \leq \Delta x_i \leq 6.5$ mm and 1.0×10^{-1} N/mm in the range $2.0 \leq \Delta x_i \leq 6.5$ mm. Although the experimental result was different from the simulation result, the spring constant of the buckled leaf spring was less than that of the weak coil spring.

Calibration of the gripping force limitation

Figure 9 shows a prototype of the forceps with the force limiter. By using the curved slider mechanism of

the proximal side, the displacement of the distal side gripper is equal to that of the proximal handle. The proximal handle was built of aluminum alloy (A5052, A6063), whereas the distal side gripper was built by 3D printing (Keyence: AGILISTA-3200, Material: AR-M2). Slide bearings (OILES # 80 flange bush) were installed in the rotating parts.

Figure 10 shows the experimental setup for gripping force measurement. The handle of the proximal side is manually driven, and a force gauge measures the maximum force on the distal side of the gripper. This test was performed 10 times, and the average gripping force was found to be 4.0 N, which was about two-thirds of the theoretical value. The variation can be attributed to friction and lack of rigidity in the transmitting mechanism.

To increase the threshold value of the gripping force, let us consider adjustment of b, after assembling the mechanism. Referring to (20), b should be set as 42 mm, which is one and a half times larger than 28 mm. Instead of adjusting b, the additional leaf spring ($(l,\ b,\ t)$=(50, 14, 0.1) mm) was installed in the gripper, as shown in Fig. 11. The gripping force increased to 6.1 N, which was approximately the same as the theoretical value.

Ex vivo experiments

Ex vivo experiments were performed to confirm that the developed forceps could limit the gripping force. A piece of chicken breast (mass: 24 g) was used as a dummy organ, and the proximal side handle was manually driven until the force limiter began to function. For comparison, a force gauge (AIKOH model RZ-20) pushed the dummy organ by using the distal gripper part.

Figure 12 shows the results of the ex vivo experiments of gripping the chicken breast when the force limiter was functioning. No slips were observed during the experiments. Figure 13 shows the chicken breast after the gripping experiments. Figure 13 also shows the damage caused by the force gauge. Minor damage to the dummy organ was observed in the gripping experiments, whereas some damage was observed where the force was greater than 11.4 N. These results indicate that the proposed method can limit the gripping force.

Discussion

Spring constant of the proposed method

The spring constant of the buckled leaf spring was estimated as 1.5×10^{-1} N/mm in the range $0.5 \leq \Delta x \leq 6.5$ mm. These results indicate that the spring constant of the proposed force limiter is less than that of a normal coil spring . Although this study examined a manual manipulator's grip, the proposed method can be applied to the joints of a surgical manipulator.

Fixation problem at the leaf spring edge

In the range $0.5 \leq \Delta x \leq 6.5$ mm, the spring constant obtained from the experiments was larger than that obtained from the simulations. However, the buckling load of the experimental value was lower than that of simulation value, as shown in Fig. 8. These findings can be attributed to the fixation method at the edges of the leaf spring. Owing to the lack of rigidity and backlash of the bearings, the angle at the edge is not always zero, as shown in Fig. 14. Both the edges cannot support momentum loads wherein Δx is is lower than a specific value, whereas they can support momentum loads wherein Δx is larger than a specific value, causing spring constant difference in simulation and experiments. The angle at the edge increases the imaginary length of the leaf springs, decreasing the buckling load.

Gripping position at the handle

In the proposed mechanism, the threshold value of the force limiter depends on the gripping position of the base and the movable handle. Thus, the threshold value error arises from the gripping position error of the handles. To reduce the threshold value error, it is expected that the handle shape reduces the gripping position error. Owing to the ease of attaching the experimental tools, the developed handle shape is straight, as shown in Fig. 9. Therefore, to reduce the gripping position error, the handle shape should be improved, as shown in Fig. 2.

Limitation of $\sigma_{\max}$

To satisfy $\sigma_{\max} < \sigma_{\lim}$, the base handle should employ a displacement limiter. Therefore, a locking mechanism can be used as the displacement limiter. Figure 15 shows the proposed locking mechanism, which is based on a traditional Japanese pothook, *Jizaikagi* [15]. If the displacement of the base handle exceeds the threshold value, the rod comes into contact with the base handle. The friction caused by this contact provides the locking mechanism, and the locking force increases with the gripping force at the handles.

Conclusions

To decrease the change in the force with respect to the displacement, the absolute value of the spring constant of a force limiter should be reduced. This paper proposed the use of a leaf spring buckling mechanism as a force limiter for forceps. The advantage of this study is the ease of adjusting the designed parameters. Specifically, the use of a leaf spring allows the thickness and width to be adjusted to the stress and force independently. Based on the simulations and experiments performed, the following findings were confirmed:

- From the simulation, the spring constant of the leaf spring was estimated as 7.9×10^{-2} N/mm, which was two-sevenths that of the weak coil spring (MISUMI AWA 8-30).
- From the experiments, the spring constant of the buckled leaf spring was estimated as 1.5×10^{-1} N/mm.
- In the calibration stage, an additional leaf spring was installed in the force limiter. This caused the threshold value of the force limiter to increase from 4.0 to 6.1 N.
- In the ex vivo experiments, minor damage to the dummy organ was observed.

These results indicate that the spring constant of the proposed force limiter is lower than that of a normal coil spring and the use of leaf spring can reduce the damage caused to the dummy organ. Additionally, locking mechanisms that can be used to limit the stress in the leaf spring, were considered. Future studies will focus on improving the force limiter mechanism and performing in vivo experiments.

Availability of Data and Materials
The datasets supporting the conclusions of this article are included within the article.

Competing interests
The author declares that he has no competing interests.

Funding
Not applicable.

Author's contributions
All work was conducted by sn.

Acknowledgements
I would like to thank Editage (www.editage.com) for English language editing.

References

1. Bodner, J., Wykypiel, H., Wetscher, G., Schmid, T.: First experiences with the da vinci operating robot in thoracic surgery. European Journal of Cardio-thoracic surgery **25**(5), 844–851 (2004)
2. Frede, T., Hammady, A., Klein, J., Teber, D., Inaki, N., Waseda, M., Buess, G., Rassweiler, J.: The radius surgical system–a new device for complex minimally invasive procedures in urology? European urology **51**(4), 1015–1022 (2007)
3. Peirs, J., Clijnen, J., Reynaerts, D., Van Brussel, H., Herijgers, P., Corteville, B., Boone, S.: A micro optical force sensor for force feedback during minimally invasive robotic surgery. Sensors and Actuators A: Physical **115**(2), 447–455 (2004)
4. Puangmali, P., Liu, H., Seneviratne, L.D., Dasgupta, P., Althoefer, K.: Miniature 3-axis distal force sensor for minimally invasive surgical palpation. IEEE/ASME Transactions on Mechatronics **17**(4), 646–656 (2012)
5. Wagner, C.R., Stylopoulos, N., Howe, R.D.: The role of force feedback in surgery: analysis of blunt dissection. In: Haptic Interfaces for Virtual Environment and Teleoperator Systems, 2002. HAPTICS 2002. Proceedings. 10th Symposium On, pp. 68–74 (2002). doi:10.1109/HAPTIC.2002.998943
6. Heimberger, R., Schaumann, U.: Forceps. Google Patents. US Patent 5,562,699 (1996). https://www.google.com/patents/US5562699
7. Sakaguchi, Y., Sato, T., Yutaka, Y., Muranishi, Y., Komatsu, T., Yoshizawa, A., Nakajima, N., Nakamura, T., Date, H.: Development of novel force-limiting grasping forceps with a simple mechanism. European Journal of Cardio-Thoracic Surgery **54**(6), 1004–1012 (2018)
8. Michelini, J., Uspenski, A., Streiff, A., John, K.R.: Grasper. Google Patents. US Patent App. 29/521,712 (2017)
9. Endo, G., Yamada, H., Yajima, A., Ogata, M., Hirose, S.: A weight compensation mechanism with a non-circular pulley and a spring: Application to a parallel four-bar linkage arm(in japanese). Journal of the Robotics Society of Japan **28**(1), 77–84 (2010)
10. Harris, R.H.: Buckling spring torsional snap actuator. Google Patents. US Patent 4,118,611 (1978). https://www.google.com/patents/US4118611
11. Lan, C.-C., Wang, J.-H., Chen, Y.-H.: A compliant constant-force mechanism for adaptive robot end-effector operations. In: Robotics and Automation (ICRA), 2010 IEEE International Conference On, pp. 2131–2136 (2010). IEEE
12. Slocum, J., Kamrin, K., Slocum, A.: A buckling flexure-based force-limiting mechanism. Journal of Mechanisms and Robotics **11**(4), 041004 (2019)
13. Beléndez, A., Pascual, C., Méndez, D., Beléndez, T., Neipp, C.: Exact solution for the nonlinear pendulum. Revista brasileira de ensino de física **29**(4), 645–648 (2007)
14. Kawauchi, M.: 2012 : AIST Database of Japanese hand size (in Japanese). https://unit.aist.go.jp/hiri/dhrg/ja/dhdb/hand/index.html
15. Noda, S.: Development of lock mechanisms using jizaikagi mechanisms for forceps force limiter. In: Proceedings of the 2019 JSME Conference on Robotics and Mechatronics, pp. 1–107 (2019). JSME

Figures

Figure 1 General force limiter mechanism.

Figure 2 Proposed forceps gripper.

Figure 3 Coordinate system of the buckled leaf spring.

Figure 4 Fixation model of the leaf spring at the edge.

Figure 5 Deformed shape of buckled leaf spring in simulation with $l_{ij} = 50$ mm and $\Delta x_i = 6.5$ mm.

Figure 6 FEM result of the stress test.

Figure 7 Experimental setup for force measurement.

Tables
Additional Files
None.

Figure 8 Simulation and experimental result of buckling force with respect to displacement. Error bars show the standard deviation.

Figure 9 Prototype force limiter.

Figure 10 Experimental setup for gripping force measurement.

Figure 11 Installation of additional leaf spring.

Figure 12 Ex vivo experiments of the force limiter.

Figure 13 Chicken breast after ex vivo experiments. Dashed lines show the gripped part and each bar represents 10 mm. (A) Force limiter. (B) 7.4 N (C) 11.4 N (D) 20.0 N.

Figure 14 Edge of the leaf spring.

Figure 15 Proposed locking mechanisms.

Table 1 Candidates of L_3 and L_4.

Candidate No.	L_3 [mm]	L_4 [mm]	l [mm]
1st candidate	24	36	70
2nd candidate	27	33	60
3rd candidate	30	30	90
4th candidate	33	27	50
5th candidate	36	24	90

Table 2 Design specification of leaf spring for the 4th candidate.

Item		Value
Δx_i	[mm]	6.5
F_i	[N]	7.37
$(t_{ij\alpha},\ t_{ij\beta})$	[mm]	(0.10, 0.11)
$(l_{ij},\ b,\ t)$	[mm]	(50, 28, 0.1)

Table 3 Simulation result of buckled leaf spring.

Item		Value
$(x(l_{ij}/2),\ y(l_{ij}/2))$	[mm]	(21.7, 11.0)
$(x(l_{ij}),\ y(l_{ij}))$	[mm]	(43.5, 0)
$\theta_{\max}$	[$^\circ$]	42.2
$(x'(l_{ij}),\ y'(l_{ij}))$		(1, 0)

Figures

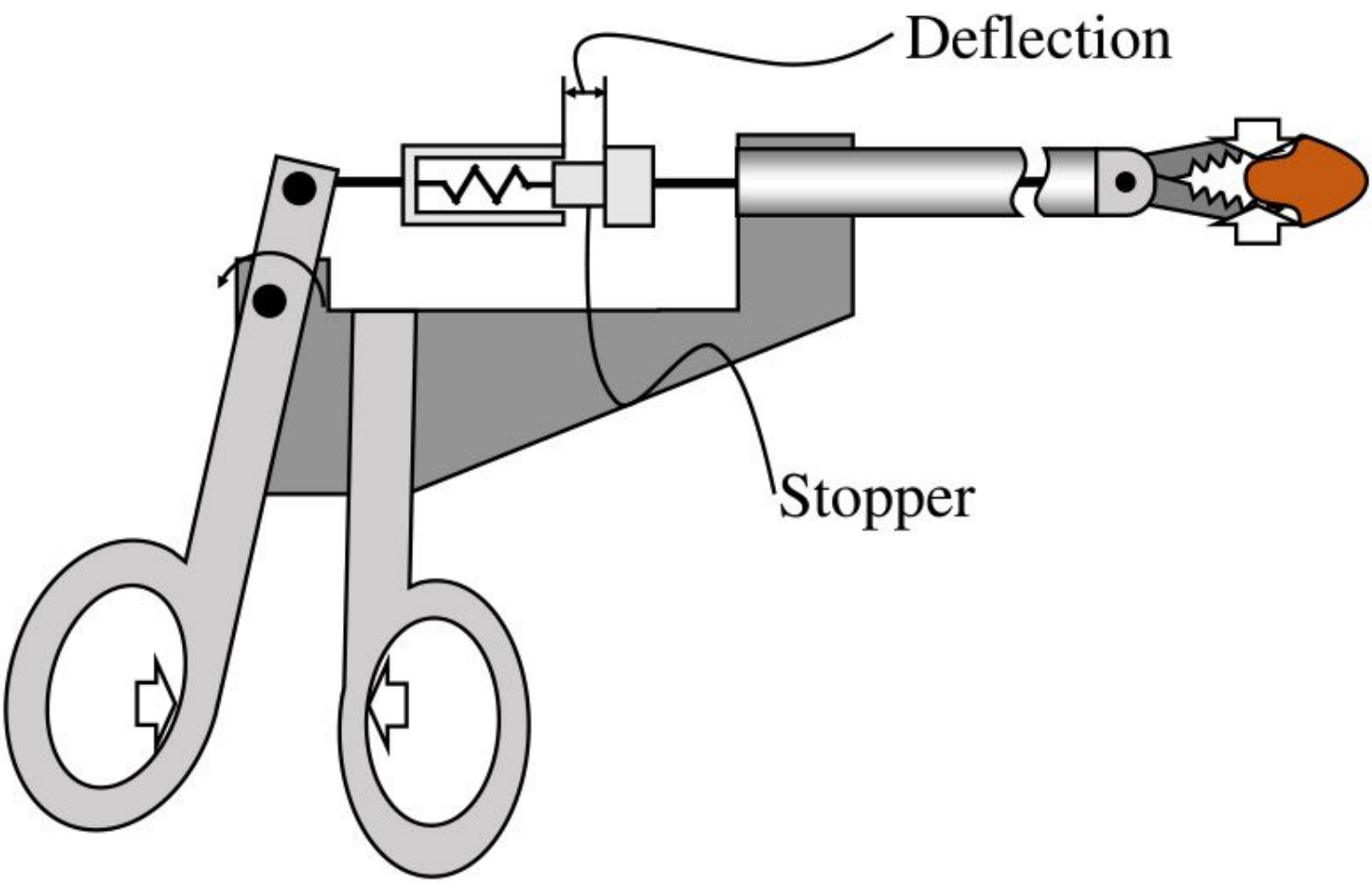

Figure 1

General force limiter mechanism.

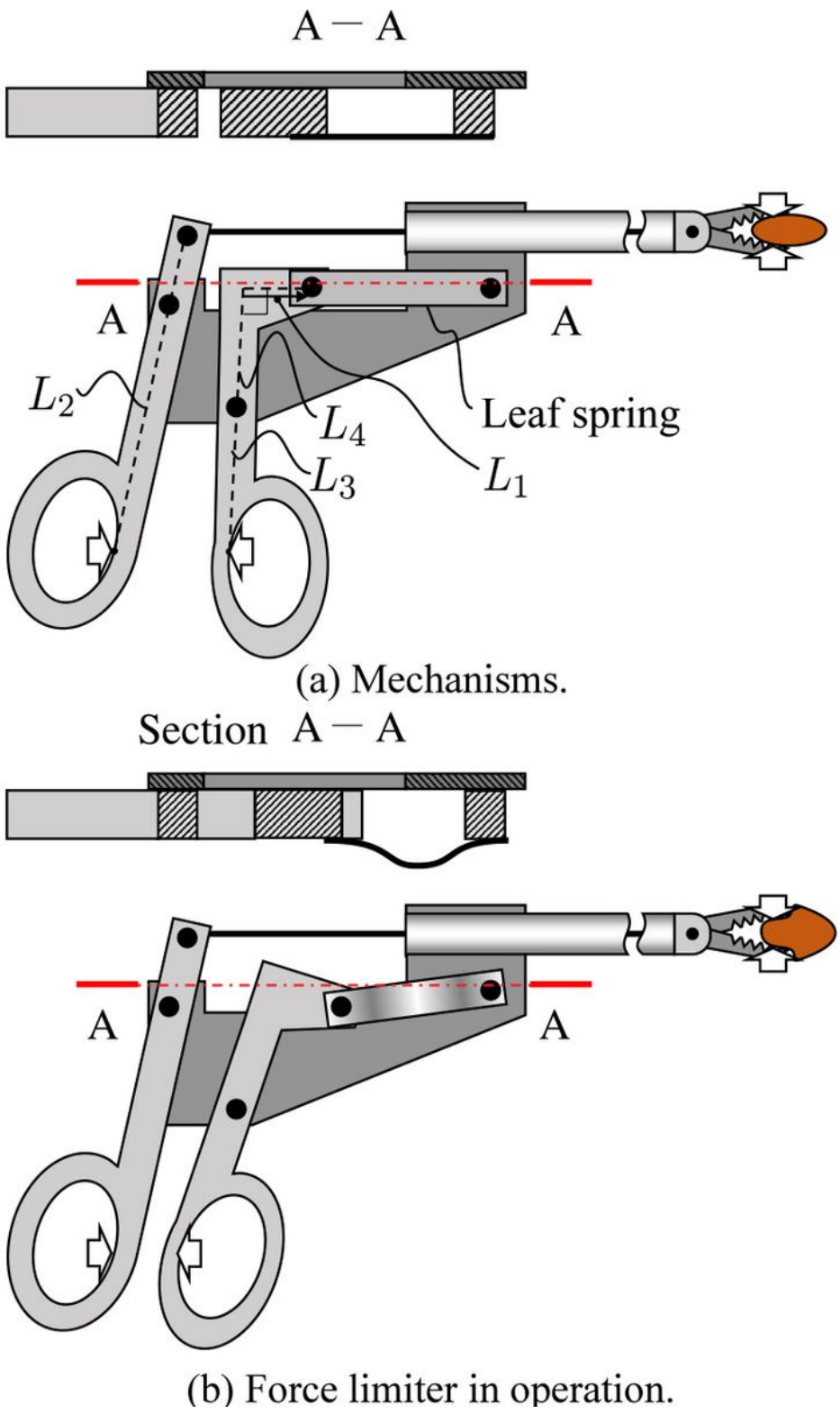

Figure 2

(a) Mechanisms. (b) Force limiter in operation. Proposed forceps gripper.

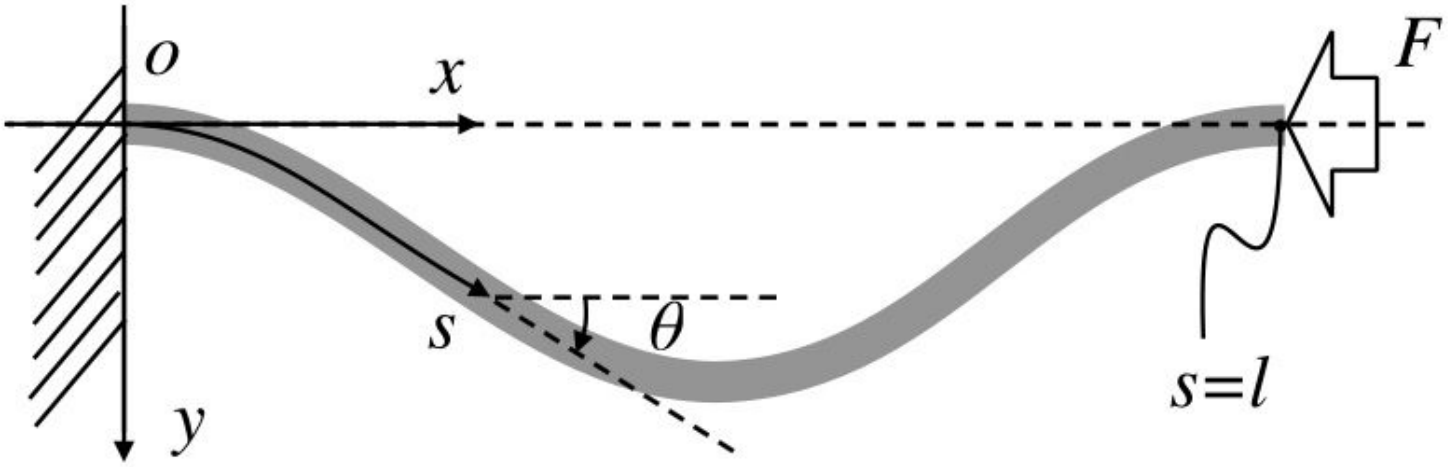

Figure 3

Coordinate system of the buckled leaf spring.

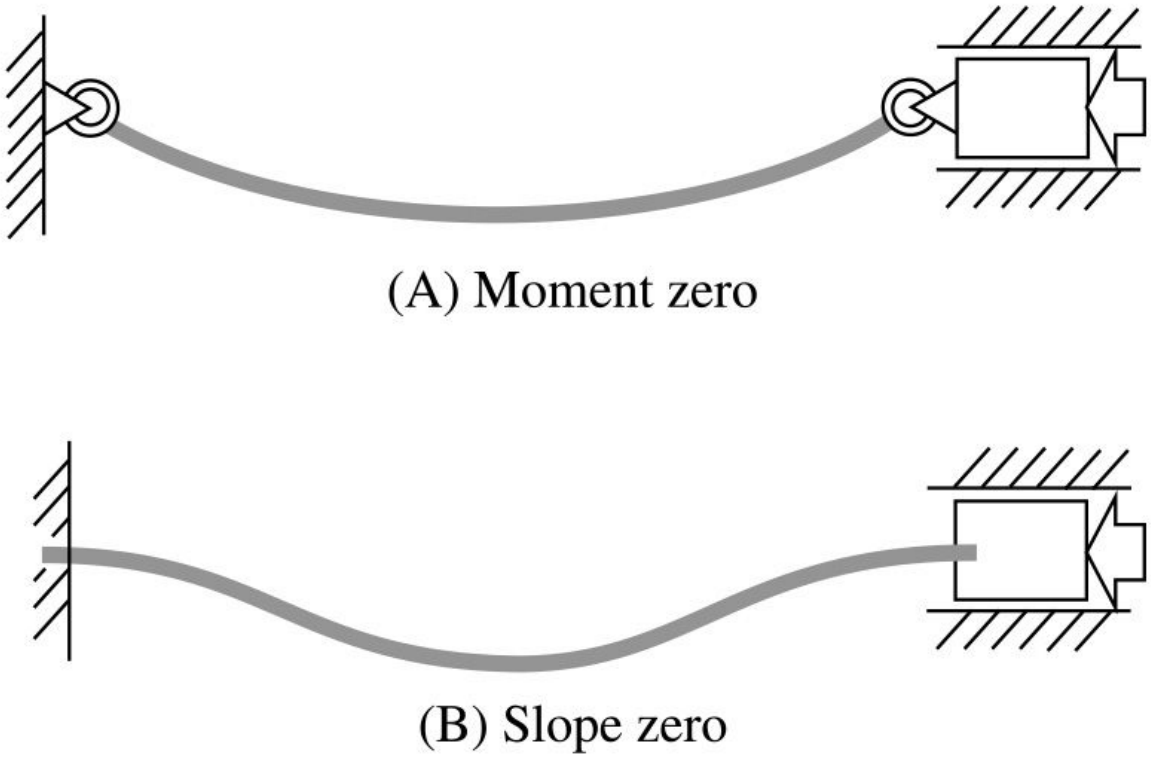

Figure 4

Fixation model of the leaf spring at the edge.

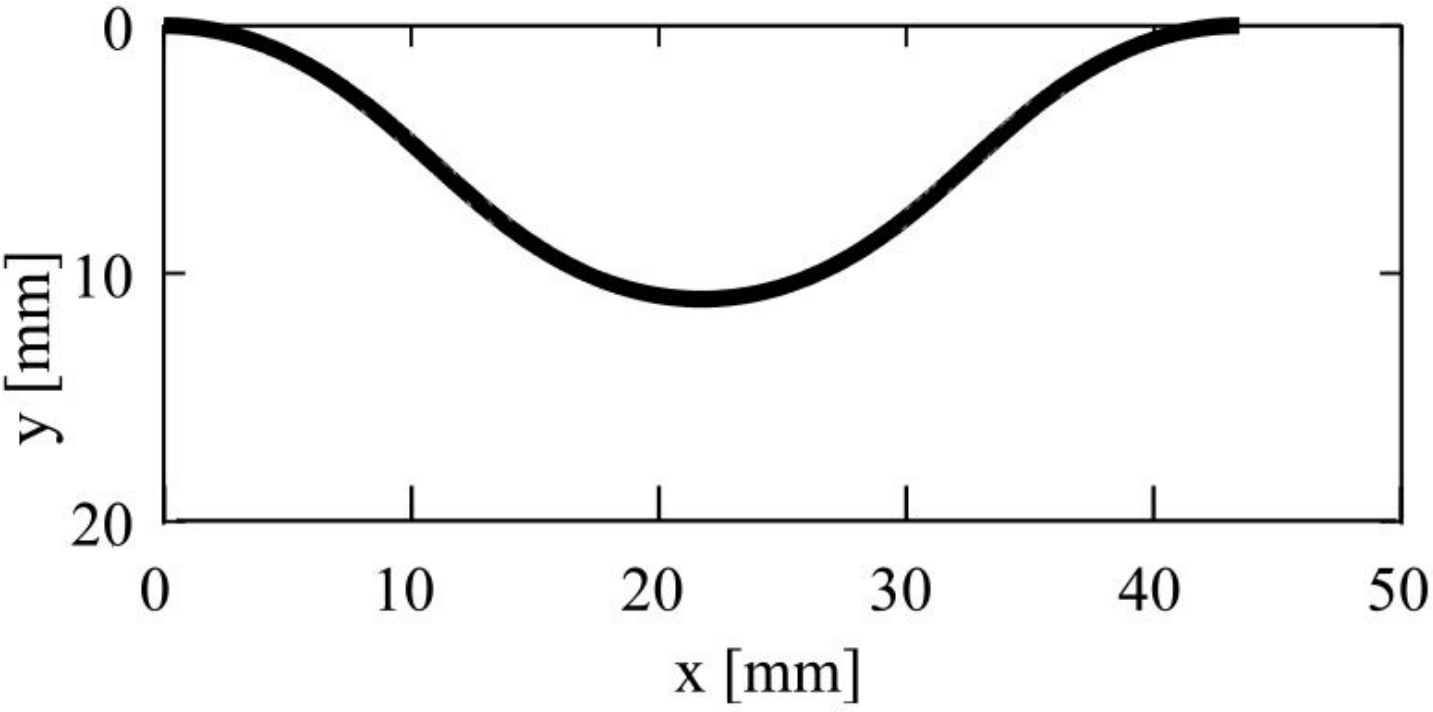

Figure 5

Deformed shape of buckled leaf spring in simulation with l_{ij}=50 mm and Delta x_i=6.5 mm.

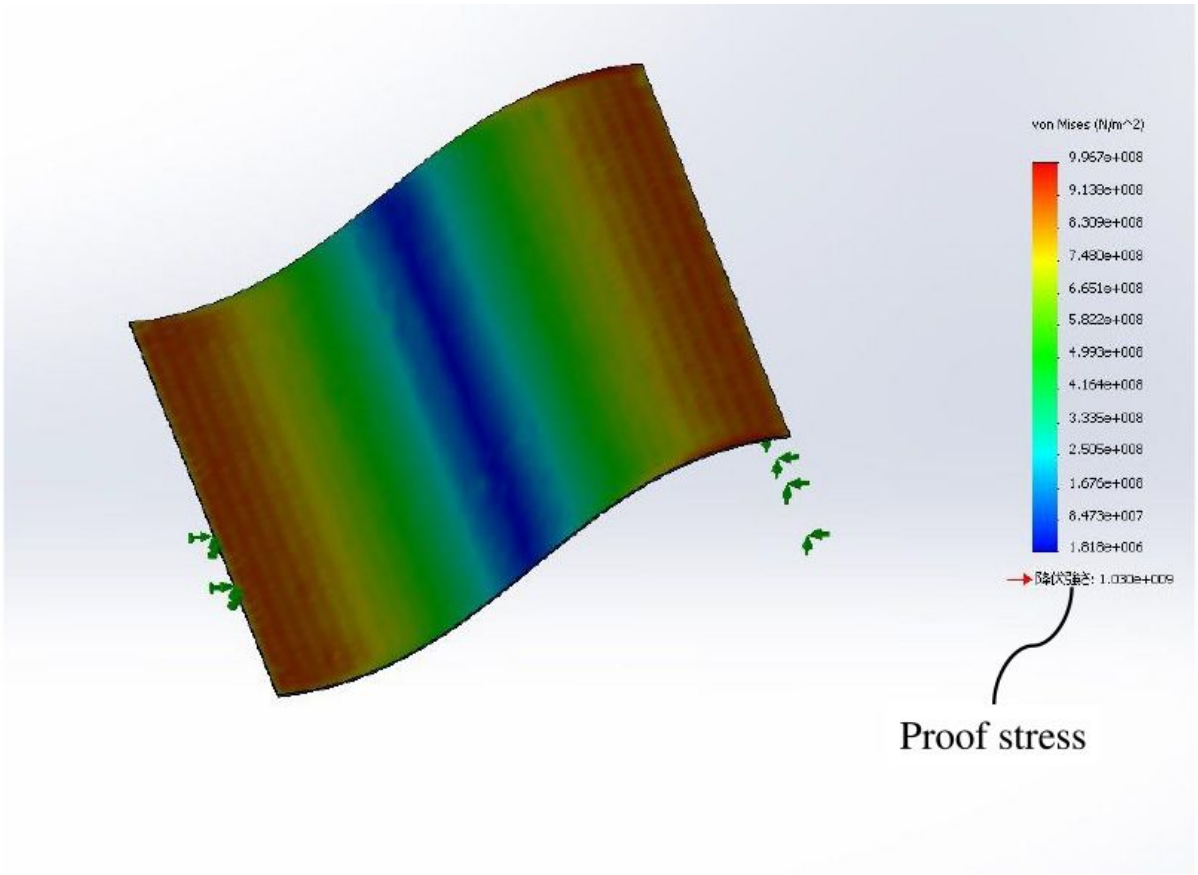

Figure 6

FEM result of the stress test.

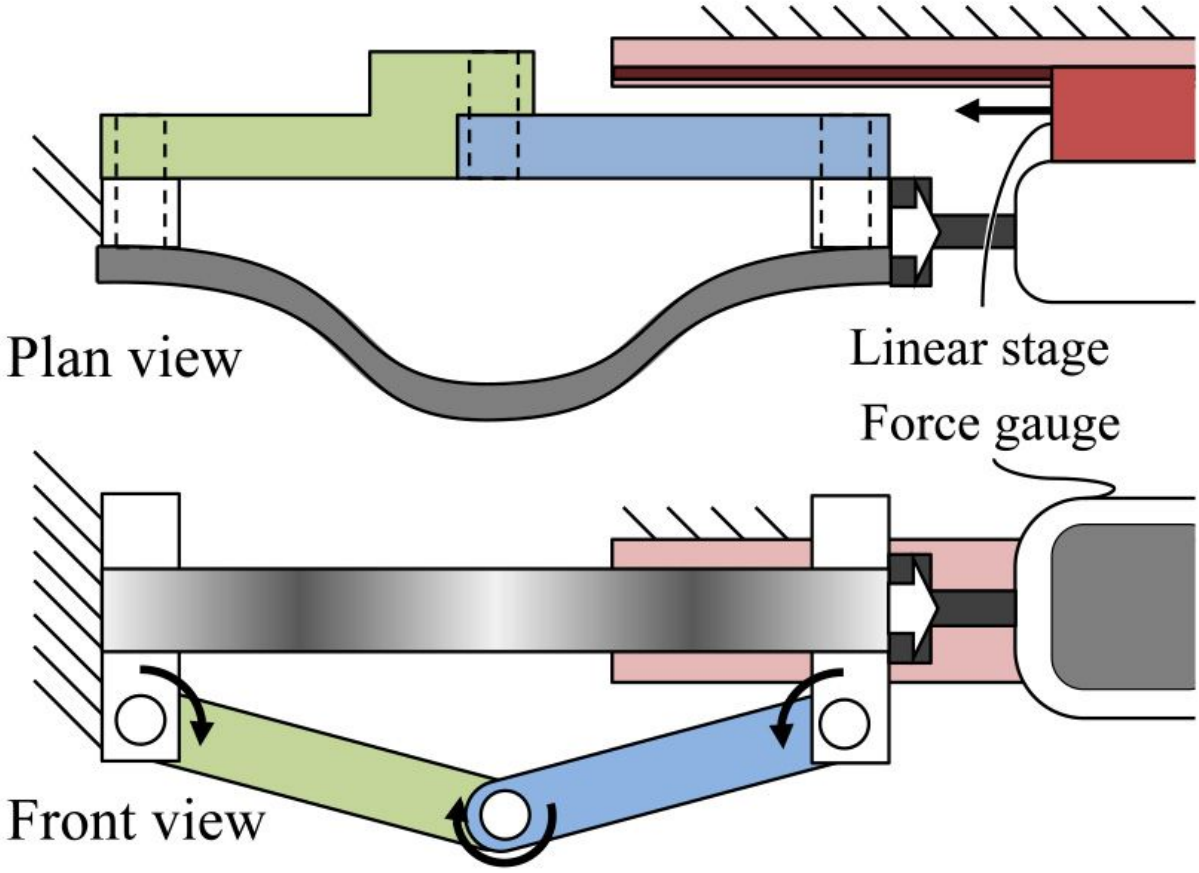

Figure 7

Experimental setup for force measurement.

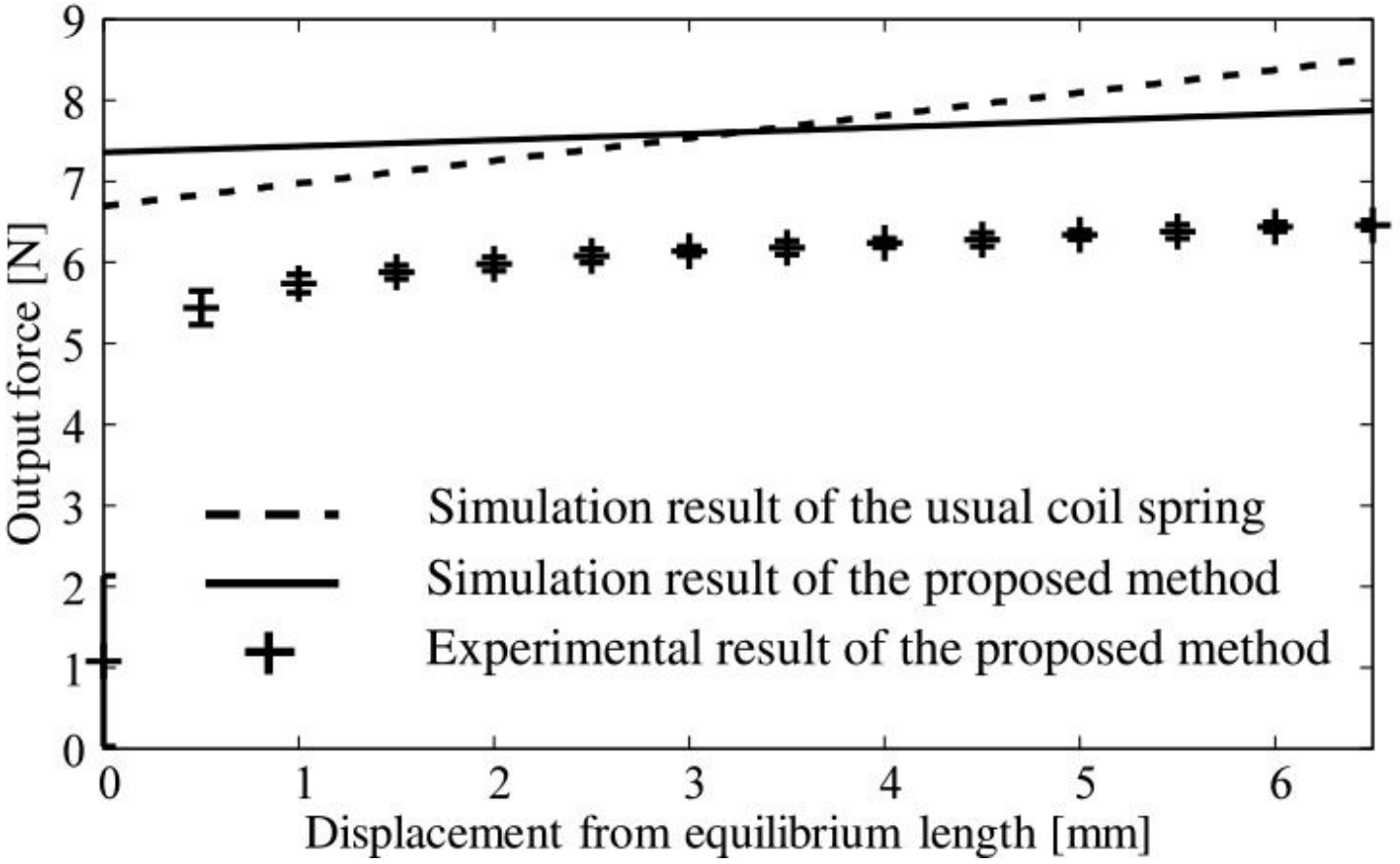

Figure 8

Simulation and experimental result of buckling force with respect to displacement. Error bars show the standard deviation.

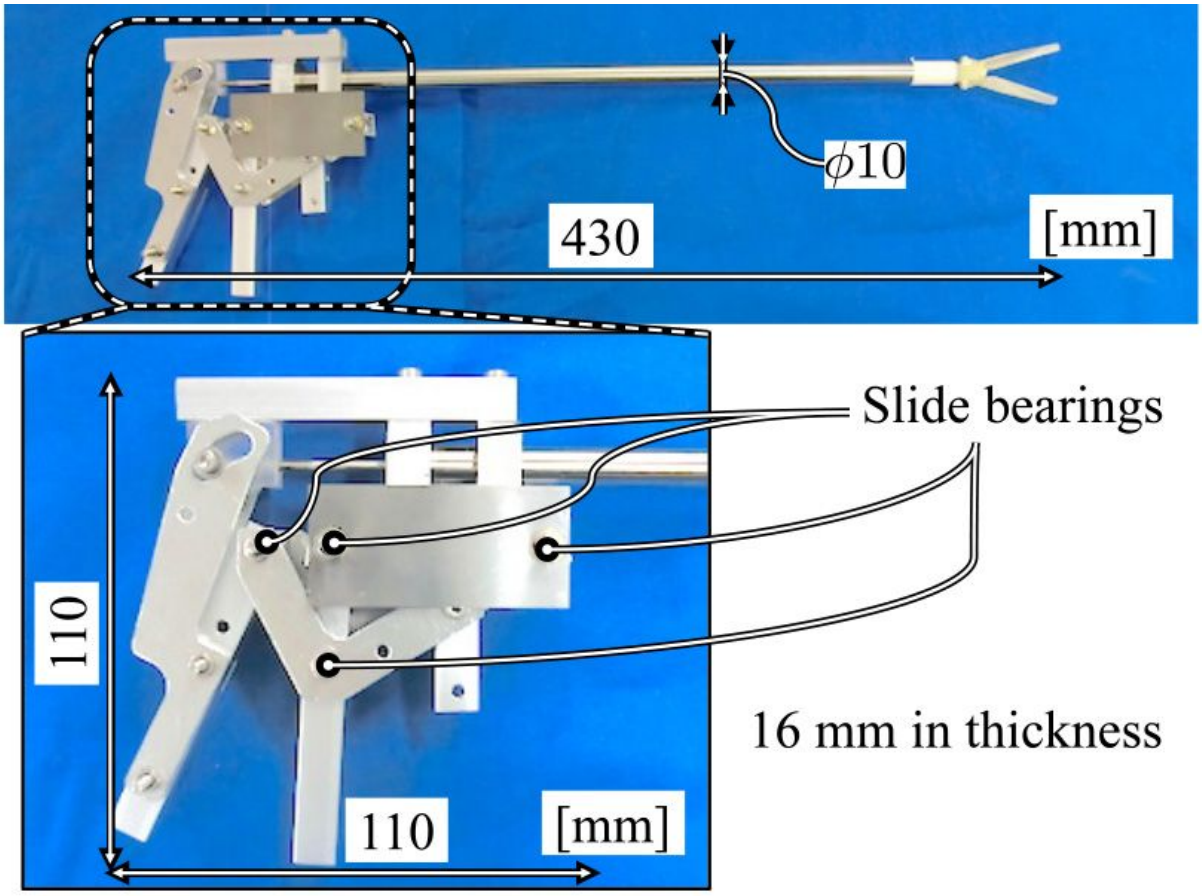

Figure 9

Prototype force limiter.

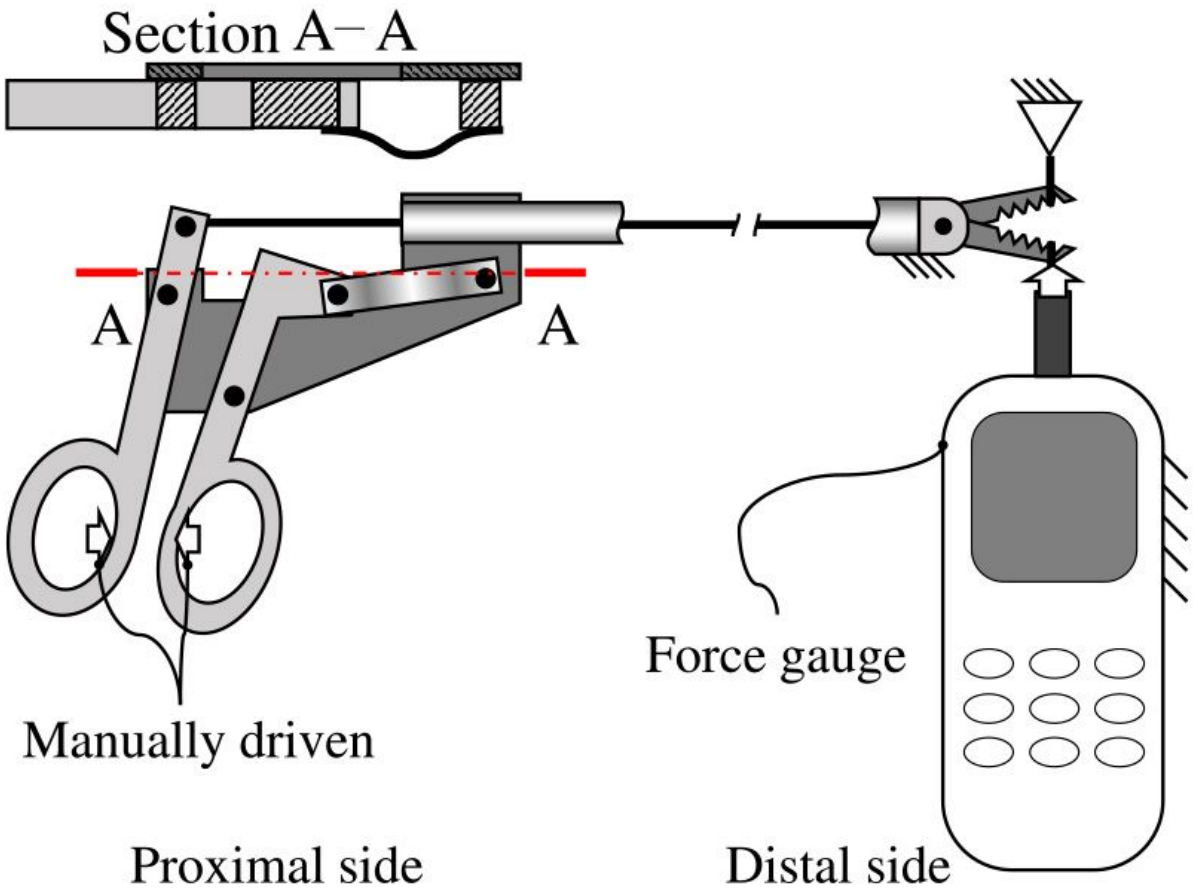

Figure 10

Experimental setup for gripping force measurement.

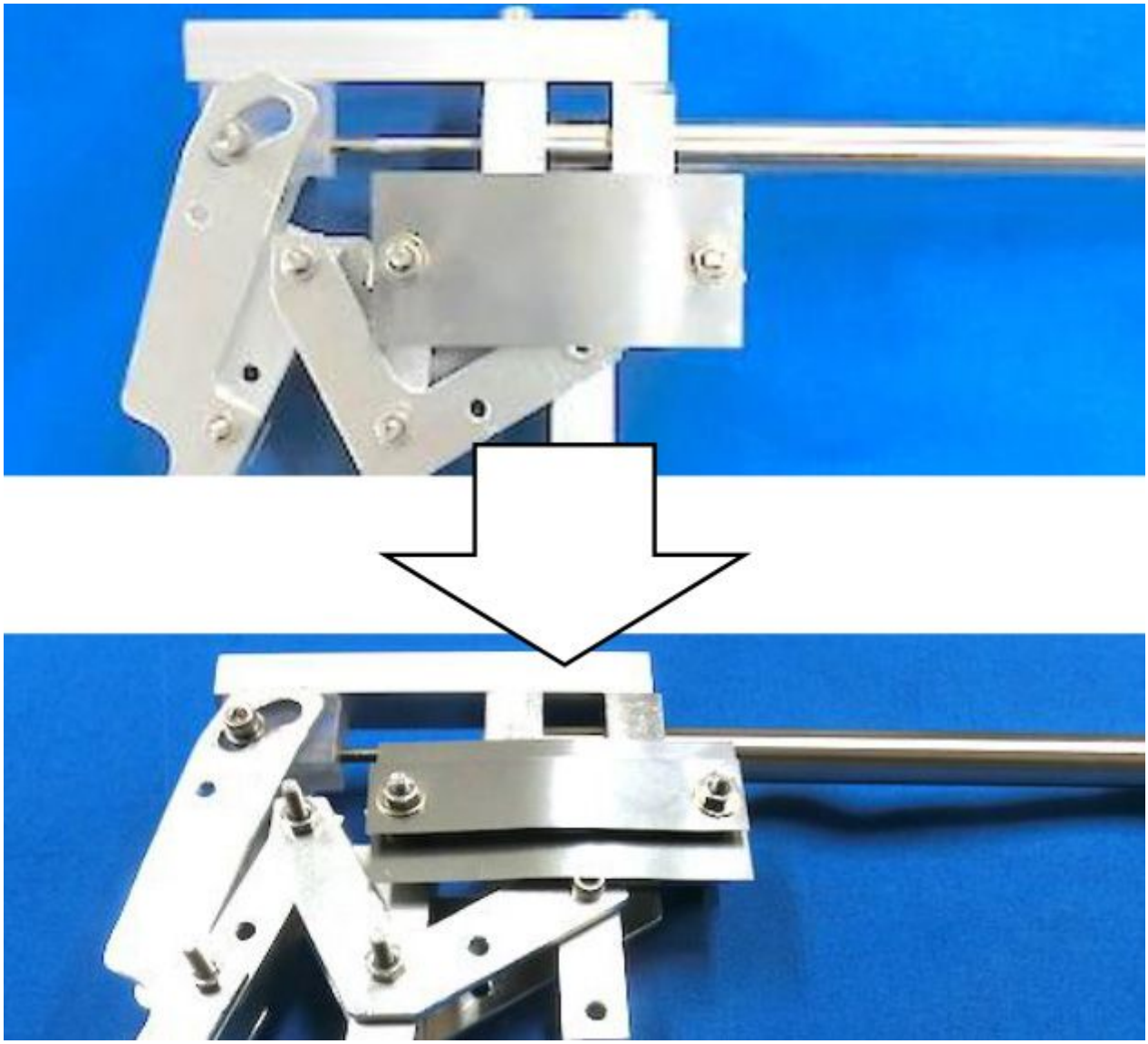

Figure 11

Installation of additional leaf spring.

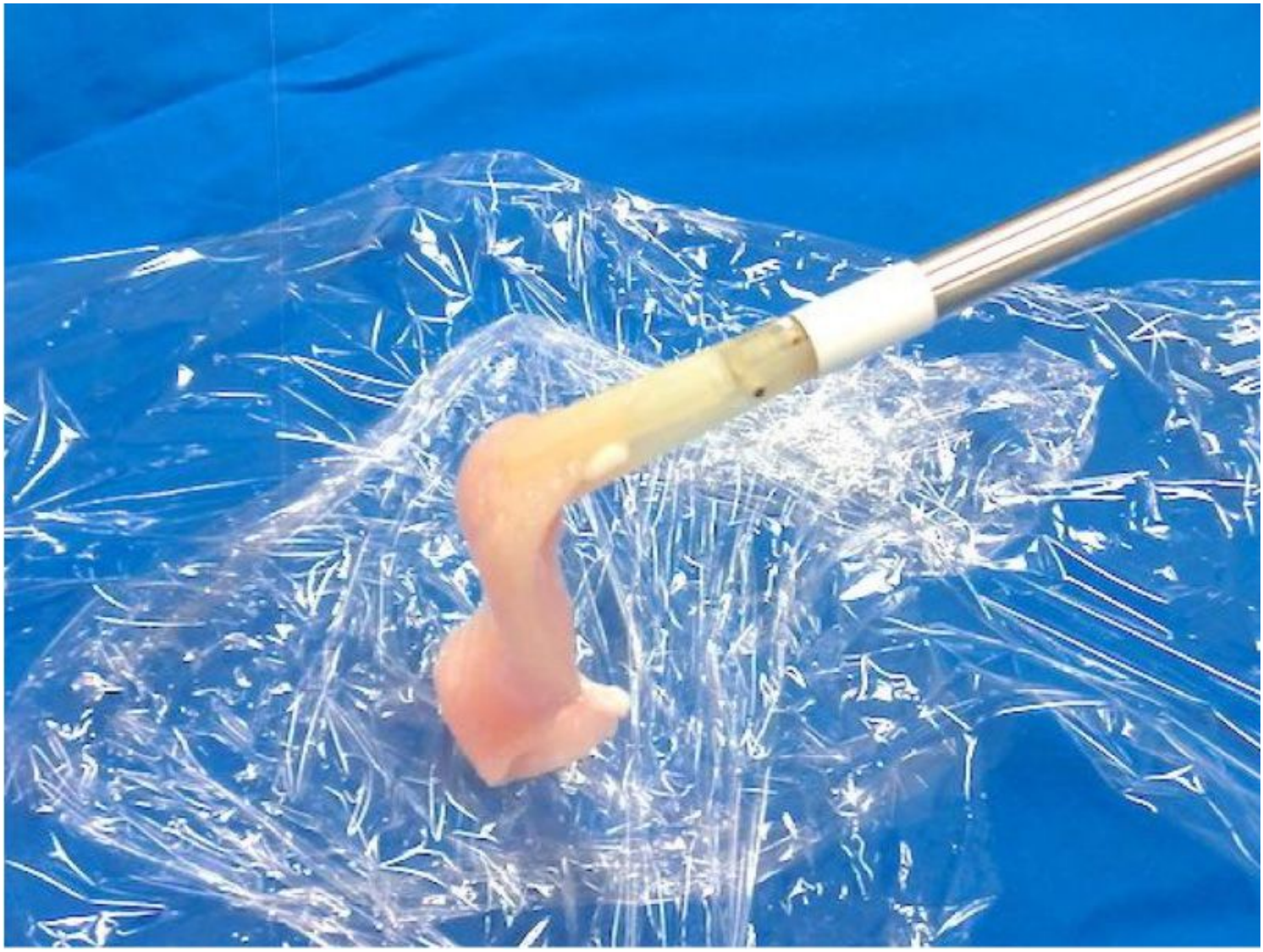

Figure 12

Ex vivo experiments of the force limiter.

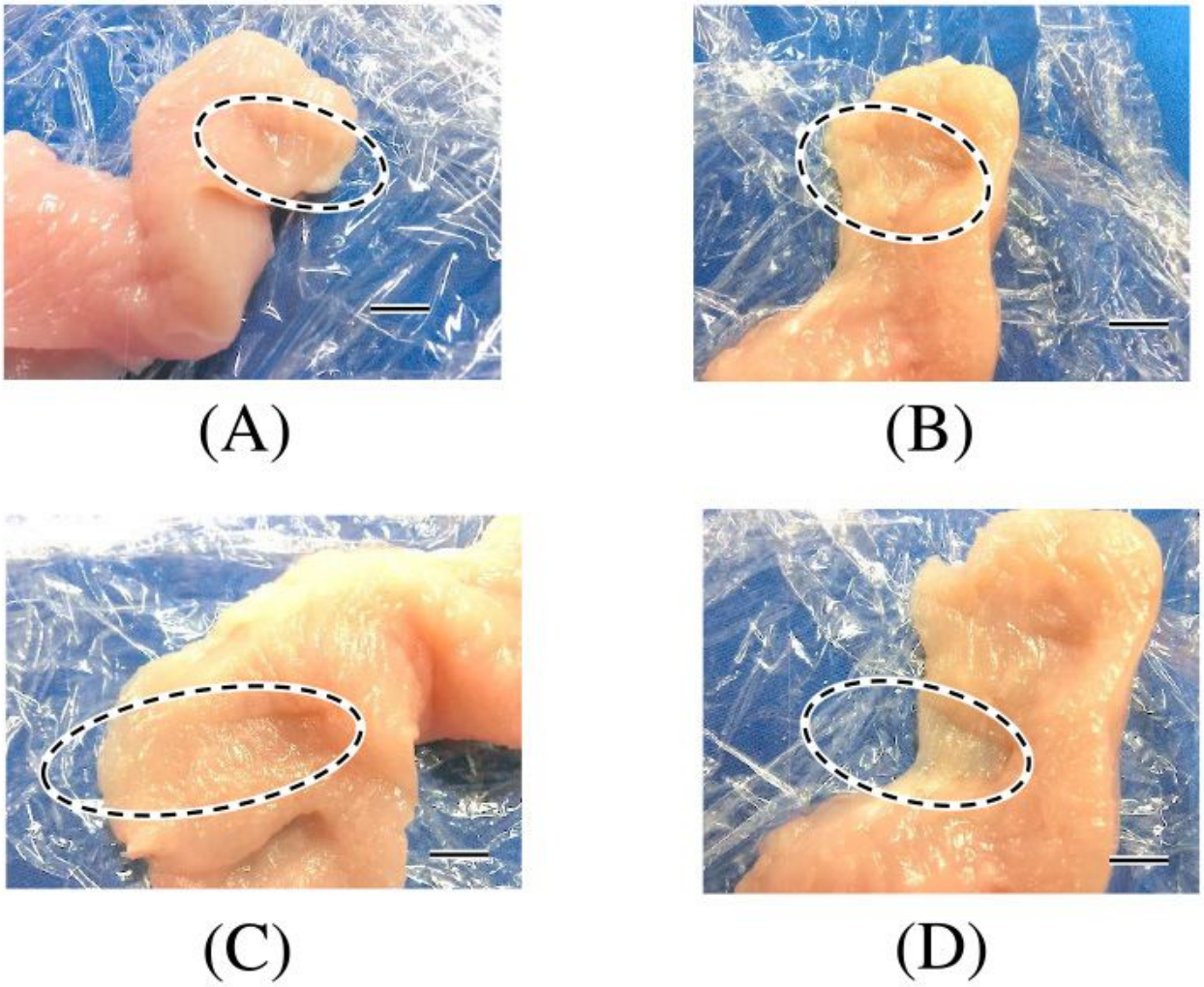

Figure 13

Chicken breast after ex vivo experiments.} Dashed lines show the gripped part and each bar represents 10~ mm. (A) Force limiter. (B) 7.4 N (C) 11.4 N (D) 20.0 N.

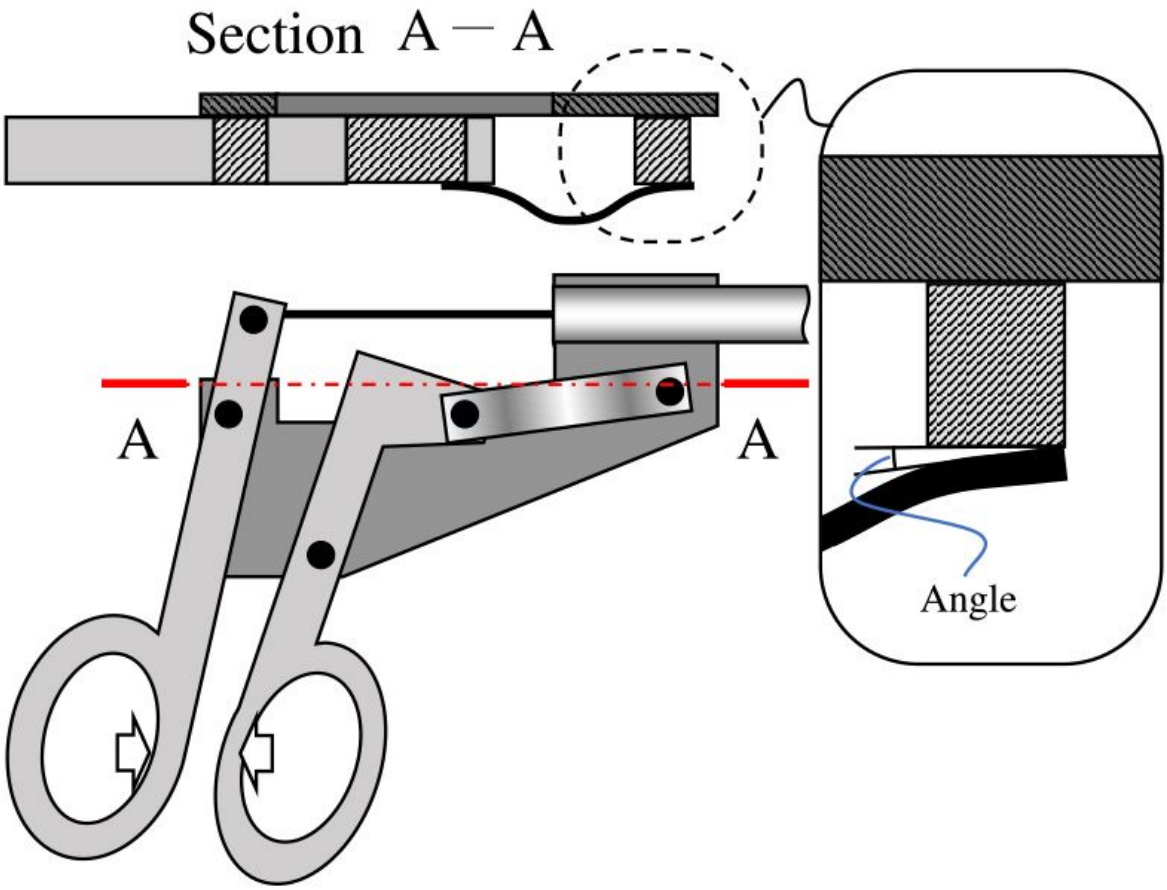

Figure 14

Edge of the leaf spring.

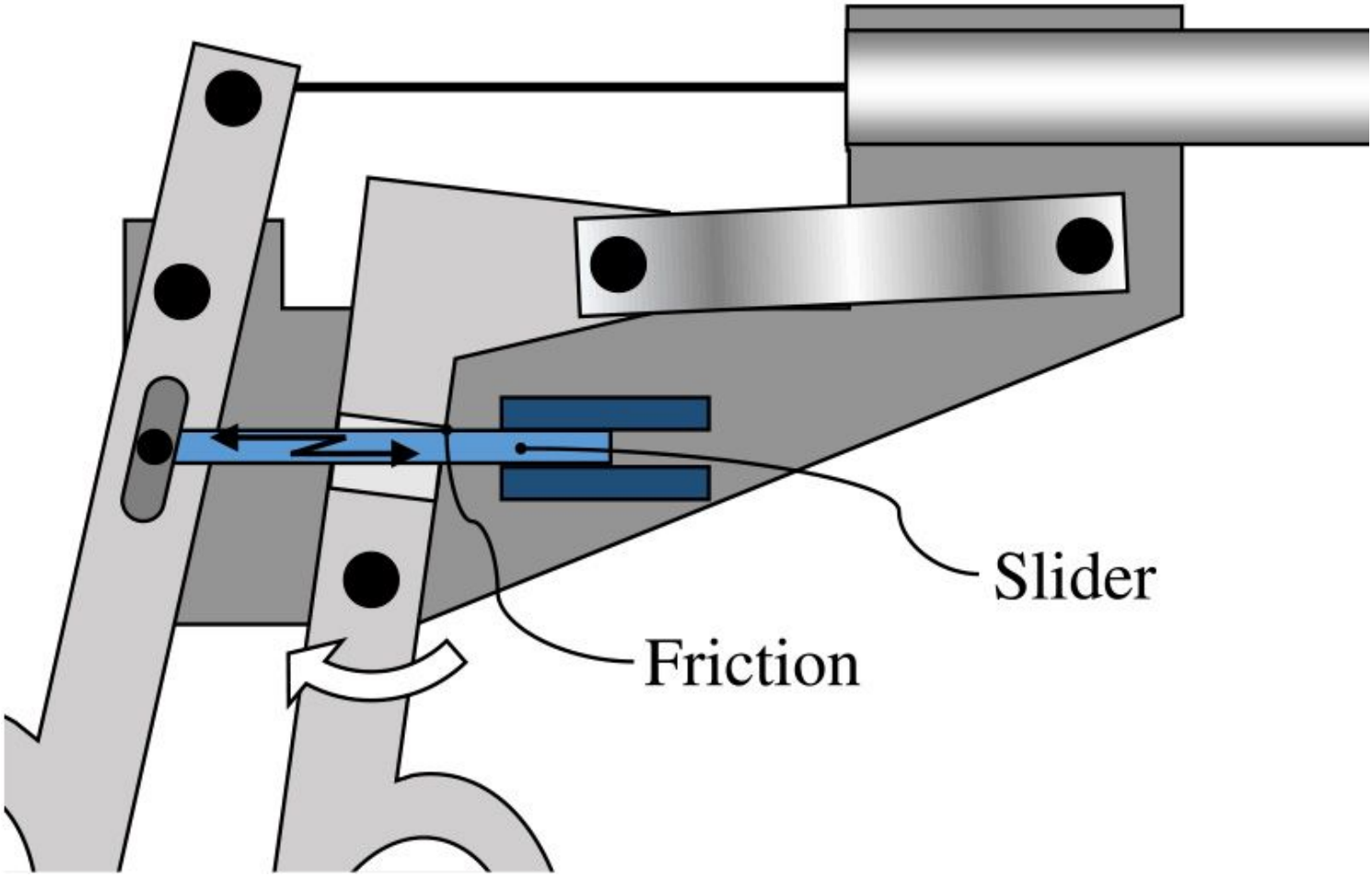

Figure 15

Proposed locking mechanisms.

Supplementary Files

This is a list of supplementary files associated with this preprint. Click to download.

- bmcarticlerev01.tex